Phase transitions of quadrupolar fluids

Seamus F. O'Shea
Department of Chemistry, University of Lethbridge, Lethbridge, Alberta, Canada, T1K 3M4

Girija S. Dubey
Brookhaven National Laboratory, Upton, New York 11973 and Department of Physics and Astronomy, Hunter College of the City University of New York, New York 10021

Jayendran C. Rasaiah
Department of Chemistry, University of Maine, Orono, Maine 04469

(Received 5 February 1997; accepted 26 March 1997)

Gibbs ensemble simulations are reported for Lennard-Jones particles with embedded quadrupoles of strength $Q^*=Q/(\epsilon\sigma^5)^{1/2}=2.0$ where ϵ and σ are the Lennard-Jones parameters. Calculations revealing the effect of the dispersive forces on the liquid–vapor coexistence were carried out by scaling the attractive r^{-6} term in the Lennard-Jones pair potential by a factor λ ranging from 0 to 1. Liquid–vapor coexistence is observed for all values of λ including $\lambda=0$ for $Q^*=2.0$, unlike the corresponding dipolar fluid studied by van Leeuwen and Smit *et al.* [Phys. Rev. Lett. **71**, 3991 (1993)] which showed no phase transition below $\lambda=0.35$ when the reduced dipole moment $\mu^*=2.0$. The simulation data are analyzed to estimate the critical properties of the quadrupolar fluid and their dependence on the strength λ of the dispersive force. The critical temperature and pressure show a clear quadratic dependence on λ, while the density is less confidently identified as being linear in λ. The compressibility is roughly linear in λ. © *1997 American Institute of Physics.* [S0021-9606(97)50625-8]

I. INTRODUCTION

Phase transitions and separations in polar fluids and polar fluid mixtures are of special importance to industrial chemists and chemical engineers. It is also of great theoretical interest to be able to characterize the nature of these coexisting phases and to pinpoint the molecular properties that lead to phase separation.

Thermodynamic perturbation theory has been the main theoretical tool in these studies in which the excess free energy $F^{\rm ex}$ is expanded about a reference system of free energy $F^{\rm ex,0}$

$$F^{\rm ex}=F^{\rm ex,0}+\zeta f_1+\zeta^2 f_2+\zeta^3 f_3+\cdots, \tag{1.1}$$

where f_1, f_2, and f_3 are integrals or the sums of integrals of the perturbing potentials of strength ζ over two- and three-body correlation functions of the reference system and the term of $O(\zeta)$ vanishes if the reference system is spherically symmetric. For example, the parameter $\zeta=\mu^2$ for a polar fluid, where μ is the dipole moment. However, the free energy expansion for dipolar and multipolar fluids oscillates widely but is tamed by the Padé approximant

$$F^{\rm ex}(\text{Padé})=F^{\rm ex,0}+\zeta^2 f_2/(1-\zeta f_3/f_2) \tag{1.2}$$

of Stell, Rasaiah, and Narang (SRN).[1] This approximation has been found to be useful in mapping the phase boundaries of simple polar fluids and their mixtures although it provides only mean-field critical exponents.

In comparing theory with experiments on real or model fluids, the reference system is often represented by the spherically symmetric Lennard-Jones potential

$$u_{ij}(r)=4\epsilon[(\sigma/r)^{12}-(\sigma/r)^6], \tag{1.3}$$

where $r=|\mathbf{r}_{ij}|$ is the distance between i and j and the perturbation is due to dipole and multipole interactions. It was thought until recently that the presence of the dispersive London term represented by $(\sigma/r)^6$ is not essential[2] since the *integrand* in f_2 is proportional to $1/r^6$. This arises from two dipole bonds in parallel with the reference correlation function $g^0(r)$ in the graphical expansion of the free energy.

It came as a surprise when Gibbs ensemble and other simulations showed the dispersive term is required and that no liquid–vapor phase transition occurs, for example, in a hard-sphere dipolar fluid.[3,4] This also implies that the application of the Padé approximant to hard spheres plus dipoles to map the coexisting phase boundaries is fundamentally flawed since it predicts phase separation. In particular, the widely quoted application of the SRN theory to dipolar hard spheres by Rushbrooke *et al.*[5] to predict the two phase region is at odds with these Gibbs ensemble simulations.

By modulating the dispersion force with a factor λ (between 0 and 1) in the pair potential

$$u_{ij}(r)=4\epsilon[(\sigma/r)^{12}-\lambda(\sigma/r)^6], \tag{1.4}$$

it was found that no phase transition occurs below $\lambda=0.35$ when the reduced dipole moment is 2.0. These results came from Gibbs ensemble simulations of a dipolar fluid.[3] Microscopic pictures of the system pinpoint the absence of a transition as due to the formation of polymers of dipolar chains when the dispersion force is weak or absent. Several other studies also seem to lend support these conclusions.[6,7] Such polymers should be absent in quadrupolar fluids and phase separation should occur at all values of λ for fluids with a sufficiently large molecular quadrupole moment.

In this paper we discuss Gibbs ensemble simulations of quadrupolar fluids over the full range of values of λ and we determine whether a liquid–vapor phase transition occurs when the dispersive force is absent (i.e., $\lambda=0$). Our results show that such phase a transition does indeed occur for a reduced quadrupole moment of $Q^*=2.0$ and the critical temperature scales quadratically with the parameter λ of the modulated Lennard-Jones reference system.

II. GIBBS ENSEMBLE SIMULATIONS OF QUADRUPOLAR FLUIDS

We have carried out Gibbs ensemble simulations of quadrupolar fluids in which the reference system is the modulated Lennard-Jones potential given in Eq. (1.4) and

$$u_{ij}^{QQ}(r)=(3Q^2/4r^5)[1-5\cos^2\theta_i-5\cos^2\theta_j-15\cos^2\theta_i \times\cos^2\theta_j+2(\cos\gamma_{ij}-5\cos\theta_i\cos\theta_j)] \quad (2.1)$$

is the quadrupolar interaction potential between molecules i and j whose relative orientation is determined by the angles (θ_i,ϕ_i) and (θ_j,ϕ_j) where $\cos\theta_i=\mathbf{e_i}\cdot\mathbf{r}_{ij}$, $\cos\theta_j=\mathbf{e_j}\cdot\mathbf{r}_{ij}$, $\gamma_{ij}=\phi_i-\phi_j=\mathbf{e_i}\cdot\mathbf{e_j}$ and $\mathbf{e_i}$ and $\mathbf{e_j}$ are unit vectors along the quadrupolar axes of i and j, respectively, and $\mathbf{r}_{ij}$ is a unit vector pointing from i to j. The reduced quadrupole moment $Q^*=Q/(\epsilon\sigma^5)^{1/2}$ where Q is the quadrupole moment and ϵ and σ are Lennard-Jones parameters.

Our implementation of the Gibbs ensemble simulation is essentially the same as that described in earlier work following the method introduced by Panagiotopoulos and co-workers.[8] The calculations were performed with 500 particles divided between two simulation boxes with nearly 350 in the liquidlike phase and the rest (150) in the vapor phase. The starting point in a run of given λ (ranging from 1.0 to 0) was a face centered cube in each box or an equilibrated sample of the two boxes at an adjacent value of λ. Similar studies of quadrupolar fluids of different strengths of the quadrupole moment Q^* have been carried successfully with the full Lennard-Jones reference potential ($\lambda=1.0$).[9,10] As in those studies, a simulation cycle consisted of attempted single particle translational and orientational displacements, followed by an attempted volume change of the boxes ($\Delta V_1=-\Delta V_2=\Delta V$) and attempted particle transfers between the boxes carried out sequentially. The translational and orientational displacements followed the usual Metropolis scheme, while the volume changes were accepted if

$$[(V_1+\Delta V)/V_1]^{N_1}[(V_2-\Delta V)/V_2]^{N_2}[-\beta(\Delta E_1+\Delta E_2)]>R, \quad (2.2)$$

where V_1 and V_2 are the box volumes, ΔV is the volume change and ΔE_1 and ΔE_2 are the corresponding energy changes and R is a random number between 0 and 1.

The particle transfers between boxes were carried out by the creation of a particle in a randomly chosen position in one box and the annihilation of a randomly chosen particle in the other box. The move was accepted if

$$[(V_1/(N_1+1))][N_2/V_2][-\beta(\Delta E_1+\Delta E_2)]>R. \quad (2.3)$$

The number of such moves was adjusted to achieve a success rate of about 1%–3%. The runs at each value of λ were carried out over at least 30 000 cycles after equilibration for 5000 cycles. The potentials were truncated at half the box length and the usual corrections applied for this cutoff in the calculation of the energy and the pressure. The chemical potential of the particles in each phase (i.e., box) was determined by Widom particle insertion method.[11] Thus the pressures (P_l,P_v) and the chemical potentials (μ_l and μ_v) are determined independently in each box while the temperatures (T_l and T_v) of the two boxes are held constant and equal to each other. The conditions for equilibrium between the phases are

$$T_l=T_v, \quad (2.4)$$

$$P_l=P_v, \quad (2.5)$$

$$\mu_l=\mu_v. \quad (2.6)$$

The last two relations are tested in the simulations. The statistical uncertainties in the average values for the liquid phases are much larger than those for the vapor phase, but otherwise the averages are consistent throughout the study, falling within the combined estimated uncertainties. Because of the larger uncertainties in the liquid values, the values used in estimating the critical vapor pressure were those for the vapor phase.

Our Gibbs ensemble simulations were carried out for quadrupolar molecules with a reduced quadrupole moment Q^* of 2.0 over the complete range of values (1.0 to 0) of the parameter λ which modulates the dispersion interaction between the molecules in Eq. (1.4). We find a liquid–gas phase transition for all values of λ including zero for this system with $Q^*=2.0$ unlike the simulations carried out by van Leeuwen and Smit, for dipolar fluids[4] with a reduced dipole moment $\mu^*=2.0$, which showed no liquid–gas phase transition for $\lambda<0.35$. Each value of λ in our study leads to a distinct coexistence curve with the coexisting densities of liquid and gas ($\rho_l^*=\rho_l\sigma^3$ and $\rho_v^*=\rho_v\sigma^3$ in reduced units) determined by the reduced temperature $T^*=kT/\epsilon$.

We have analyzed the coexistence curves at each λ assuming the law of rectilinear diameters and

$$(\rho_l^*+\rho_v^*)/2=A(T_c^*-T^*)+B, \quad (2.7)$$

and a scaled coexistence curve of the form

$$(\rho_l^*-\rho_v^*)=C|1-T^*/T_c^*|^\beta, \quad (2.8)$$

where $\beta=0.32$, ρ_c^* and T_c^* are the reduced density and temperature, respectively, at the critical point and A, B, and C are constants. The critical pressures were determined by fitting $\ln P^*$ linearly in $1/T^*$. Our results are summarized in Table I and are plotted in Figs. 1–5.

Gibbs ensemble calculations for Lennard-Jones fluids show negligible size effects, whereas those for square well fluids show marked finite size effects.[12] In the present case we have tested the size dependence by comparing calculations for $N=500$, 1000, and 1200. Except near the critical point, where the larger systems are more stable due to the $N^{-1/2}$ effect, no systematic differences are evident in the

TABLE I. Data for coexisting phases as a function of the damping factor λ of the damped Lennard-Jones fluid with embedded linear quadrupoles ($Q^* = 2$). Asterisks mean this data set has not been used in determining ρ_c.

	T	ρ_l	ρ_v	P_l	P_v	E_l	E_v	μ_l	μ_v
λ = 0	1.2	0.657	0.0053	0.0103	0.0059	−12.6374	−0.8923	−4.8758	−6.673
	1.25	0.623	0.0075	0.0122	0.0088	−12.1527	−1.0116	−7.2874	−6.508
	1.3	0.6152	0.0167	0.0148	0.0159	−11.7673	−2.0188	−5.0608	−6.1971
	1.35	0.5533	0.0217	0.0179	0.0207	−11.0302	−2.035	−4.5946	−6.1538
	1.4	0.5244	0.0438	0.0297	0.0337	−10.5065	−3.2422	−4.1651	−5.7271
	1.35	0.5484	0.0204	0.0209	0.0194	−11.0581	−2.0221	−5.2339	−6.0074
	1.3	0.6071	0.0149	0.0144	0.014	−11.6971	−1.858	−8.3835	−6.0767
	1.4	0.532	0.0391	0.0302	0.0329	−10.5888	−2.9961	−5.2313	−5.8558
	1.425	0.4837	0.0642	0.0428	0.0412	−10.0459	−4.2192	−4.9804	−5.482*
	1.45	0.4586	0.081	0.0477	0.0489	−9.6892	−4.6042	−5.2212	−5.3479*
	1.475	0.3748	0.1224	0.0572	0.0593	−8.8164	−5.4912	−4.8794	−5.3843*
	1.5	0.3003	0.1849	0.0707	0.0706	−7.9369	−6.5913	−5.6126	−5.1602*
λ = 0.1	1.3	0.7357	0.0054	0.0152	0.0065	−14.0628	−0.8934	−7.4114	−7.0948
	1.4	0.6744	0.0123	0.0241	0.015	−13.083	−1.4619	−4.9046	−6.7006
	1.45	0.6453	0.0198	0.0292	0.021	−12.5719	−1.9774	−5.6023	−6.4558
	1.5	0.6098	0.0283	0.0316	0.0292	−11.9774	−2.3294	−5.4291	−6.36
	1.55	0.5776	0.0428	0.0438	0.0408	−11.4389	−2.897	−5.9503	−6.0339
	1.6	0.4951	0.0624	0.0578	0.0541	−10.4225	−3.6224	−5.3355	−5.948
	1.6	0.5052	0.065	0.0562	0.0551	−10.5319	−3.7092	−5.2774	−6.7383
	1.65	0.4153	0.1519	0.0818	0.0803	−9.4068	−5.982	−5.4987	−5.6052
λ = 0.2	1.55	0.7202	0.0145	0.0282	0.0179	−14.1378	−1.431	−7.2536	−7.2132
	1.6	0.697	0.0214	0.0291	0.0256	−13.679	−1.92	−7.0125	−7.0683
	1.65	0.6648	0.0312	0.0436	0.0359	−13.1089	−2.4702	−5.9355	−7.0442
	1.7	0.6198	0.0421	0.049	0.0462	−12.4163	−2.7685	−6.1703	−6.5726
	1.75	0.5795	0.0604	0.0641	0.0622	−11.7725	−3.4688	−6.1104	−6.3758
	1.775	0.5527	0.0797	0.0727	0.0705	−11.3885	−4.2786	−6.1224	−6.3413
	1.8	0.5223	0.108	0.0837	0.0847	−10.9226	−4.9814	−5.8423	−6.2526
	1.825	0.4904	0.1302	0.0935	0.0932	−10.4605	−5.5014	−6.0085	−6.1787
	1.85	0.4491	0.2004	0.1097	0.1063	−9.8889	−6.7846	−5.9093	−6.016*
λ = 0.4	1.9	0.7862	0.0189	0.0318	0.0284	−16.2846	−1.5484	−6.8202	−7.9657
	2	0.7383	0.0335	0.0558	0.0503	−15.3103	−2.3014	−6.8513	−7.9245
	2	0.7334	0.0325	0.0465	0.0487	−15.2315	−2.138	−6.5127	−7.9005
	2.1	0.6716	0.0565	0.0828	0.0777	−14.0163	−3.0441	−7.157	−7.5526
	2.15	0.6358	0.0809	0.1103	0.1022	−13.4037	−3.8808	−6.8561	−7.2691
	2.2	0.5909	0.1097	0.1266	0.1233	−12.5842	−4.703	−7.2146	−7.1076
	2.225	0.5604	0.1273	0.1403	0.1367	−12.1169	−5.1183	−7.1361	−6.9827
	2.25	0.4536	0.1871	0.1479	0.151	−10.7151	−6.6166	−6.8687	−7.0792*
	2.25	0.5216	0.1994	0.1592	0.1483	−11.5344	−6.8342	−6.6781	−6.8589*
λ = 0.6	2.4	0.8063	0.0352	0.0648	0.0657	−17.7944	−2.1093	−8.8223	−9.1636
	2.5	0.75	0.055	0.0995	0.0966	−16.55	−2.93	−7.56	−8.77
	2.55	0.7215	0.0654	0.1228	0.1133	−15.942	−3.194	−8.6183	−8.7212
	2.6	0.6855	0.0866	0.1334	0.14	−15.214	−3.863	−9.0592	−8.4257
	2.65	0.6564	0.1118	0.1792	0.1675	−14.2252	−4.36	−9.3223	−8.348
	2.7	0.6145	0.1329	0.2078	0.1946	−13.8074	−4.9279	−7.8632	−8.0493
	2.75	0.519	0.1808	0.227	0.2299	−12.243	−5.9657	−8.0146	−7.8933
λ = 0.8	2.9	0.8403	0.0427	0.0938	0.0963	−19.9197	−2.3306	−9.9336	−10.5181
	2.95	0.8238	0.0552	0.1163	0.1188	−19.4404	−2.8422	−10.0918	−10.1994
	3	0.802	0.0639	0.1447	0.137	−18.9021	−3.0718	−10.7762	−10.0379
	3.05	0.7727	0.0739	0.1507	0.1545	−18.2159	−3.4259	−11.1136	−9.9215
	3.1	0.7428	0.0843	0.1791	0.1756	−17.5518	−3.7433	−9.4762	−9.8261
	3.15	0.7162	0.1066	0.2142	0.207	−16.8925	−4.4262	−9.3484	−9.5981
	3.2	0.696	0.1463	0.2484	0.248	−16.3953	−5.7755	−8.9094	−9.2875
	3.25	0.6289	0.1452	0.2661	0.2658	−15.103	−5.3403	−9.2495	−9.4063
	3.2	0.6888	0.1381	0.2516	0.2408	−16.2497	−5.4441	−9.3215	−9.398
	3.25	0.6508	0.2096	0.288	0.2876	−15.4878	−7.4878	−9.6555	−9.254
λ = 1.0	3.3	0.9427	0.0339	0.1025	0.0932	−24.1964	−1.9815	−11.5415	−12.3851
	3.4	0.9083	0.0463	0.1203	0.1232	−23.1952	−2.4941	−11.6241	−11.9623
	3.5	0.8661	0.0592	0.1571	0.1552	−21.9932	−3.0092	−11.1249	−11.7416
	3.6	0.8358	0.0852	0.2031	0.2078	−21.0482	−3.9718	−10.7642	−11.24
	3.7	0.7895	0.1107	0.2807	0.2599	−19.831	−4.6374	−11.3005	−10.9847
	3.8	0.7313	0.1467	0.3255	0.3208	−18.4064	−5.708	−10.6174	−10.7286
	3.9	0.6427	0.218	0.4001	0.3999	−16.428	−7.6987	−10.4674	−10.4598

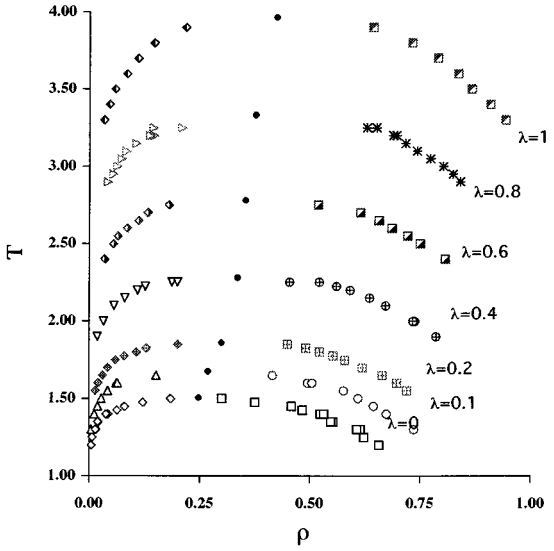

FIG. 1. Coexistence curves of the liquid and vapor densities in reduced units as a function of the reduced temperature T^* of a quadrupolar fluid ($Q^*=2.0$) for different values of λ which modulates the dispersive term of the Lennard-Jones reference system—see Eq. (1.4).

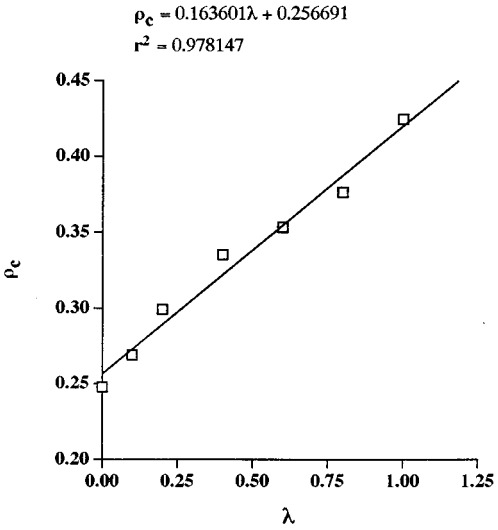

FIG. 3. Plot of the critical density ρ_c^* vs λ for a modulated Lennard-Jones quadrupolar fluid with $Q^*=2.0$. The equation gives the best least-squares linear fit to the data.

results, and so all data for all system sizes are used in determining the critical constants reported in Table II. The data for T_c^* and P_c^* are very stable and well behaved, having $r^2>0.99$ in almost every case. The data for ρ_c^* on the other hand, are less well behaved and show scatter especially near T_c^*. These results are somewhat surprising, because it means the difference in the densities is better behaved than the sum; the variation shown is small but significant relative to the systematic variation in ρ_c^* as a function of λ, as may be seen in Fig. 3. A careful examination of block averages, obtained by partitioning the production runs into 500 cycle blocks, shows that the relaxation ''time'' for the densities is long, necessitating long runs. Most of the results reported here are for averages over 50 000 cycles, although a few are for shorter runs; in those cases the results are for stable parts of runs where the boxes switched identities as they sometimes do near T_c^*.

III. DISCUSSION

As expected, the vapor–liquid equilibrium of the quadrupolar LJ fluid is more like that of the pure LJ fluid than that of the dipolar damped LJ fluid[3,4,6,7] where the liquid–gas phase transition is believed to be inhibited by chain formation below a limiting value of λ. The problem however is

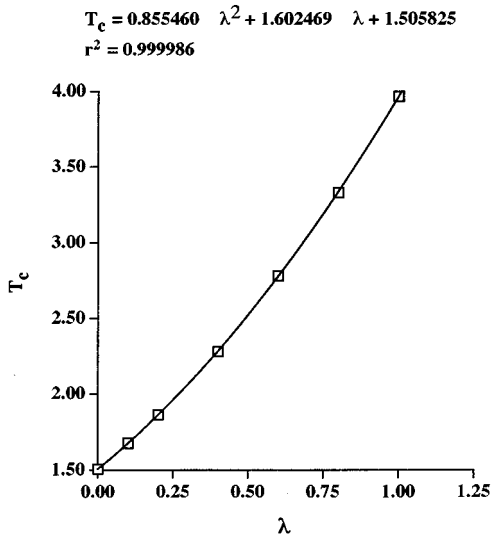

FIG. 2. Plot of the critical temperature T_c^* vs λ for a modulated Lennard-Jones quadrupolar fluid with $Q^*=2.0$. The equation gives the best least-squares quadratic fit to the data.

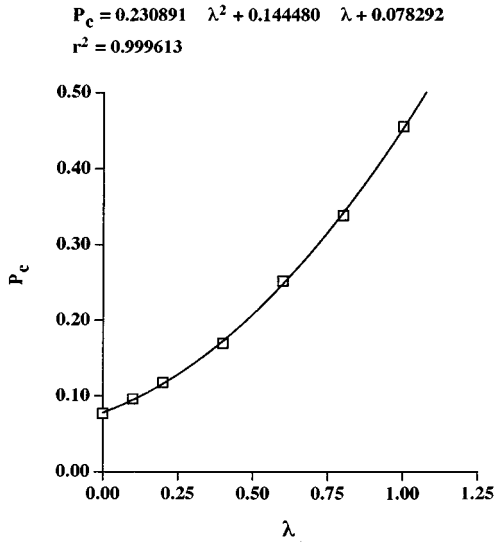

FIG. 4. Plot of the critical pressure P_c^* vs λ for a modulated Lennard-Jones quadrupolar fluid with $Q^*=2.0$. The equation gives the best least-squares quadratic fit to the data.

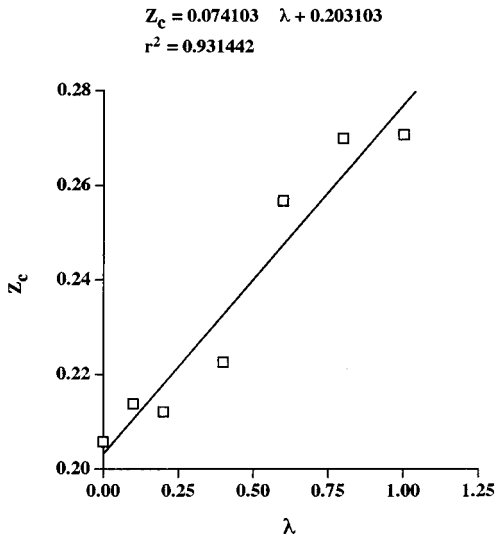

FIG. 5. Plot of the critical compressibility Z_c^* vs λ for a modulated Lennard-Jones quadrupolar fluid with $Q^*=2.0$. The equation gives the best least-squares linear fit to the data.

more subtle than generally realized since the modulated reference potential can be rewritten as

$$u(r)=4\epsilon'[(\sigma'/r)^{12}-(\sigma'/r)^{6}], \tag{3.1}$$

where $\epsilon'=\epsilon\lambda^2$ and $\sigma'=\sigma/\lambda^{1/6}$ showing that it is still a two parameter Lennard-Jones potential so long as $\lambda\neq 0$. This suggests that the phase transition (or lack thereof) in dipolar fluids is related to the strength of the dipole moment relative to the depth of the Lennard-Jones potential well. A strong enough dipole moment will prevent the Lennard-Jones liquid–gas phase transition by promoting chain formation. The critical value of this ratio remains to be determined empirically (computer simulation!) or by theoretical analysis. The competition between chain association and liquid condensation has been studied in the context of a van der Waals mean-field theory by van Roij[13] and the effect of molecular elongation of dipolar hard-core spherocylinders on this competition has been investigated by McGrother and Jackson[14] using computer simulation.

In the absence of dipole or multipolar interactions, the intermolecular potential has the Lennard-Jones form Eq. (3.1) when $\lambda\neq 0$, and systems with different values for the parameters ϵ' and σ' in Eq. (3.1) obey the law of corresponding states. The configurational free energies $F(V,T;\lambda)$ of two such systems are related by[15]

$$F(V,T;\lambda)=\lambda^2 F(V',T';\lambda=1)+(NkT/2)\ln\lambda, \tag{3.2}$$

where $V'=V\lambda^{1/2}$ and $T'=T/\lambda^2$. Differentiation with respect to the volume relates the single phase pressures by

$$P(V,T;\lambda)=\lambda^{5/2}P(V',T';\lambda=1). \tag{3.3}$$

The equations of state are also related using appropriate scaled variables,[14] but the reduced critical density $\rho_c\sigma'^3$, critical temperature kT_c/ϵ' and critical pressure $P_c\sigma'^3/\epsilon'$ are unchanged.

In our study we define the reduced density, temperature, and pressure for all λ by $\rho^*=\rho\sigma^3$, $T^*=kT/\epsilon$ and $P^*=P\sigma^3/\epsilon$, respectively, where σ and ϵ are the parameters of the unmodulated Lennard-Jones potential i.e., for $\lambda=1$. It follows that the reduced critical temperature T_c^* scales as λ^2 and the reduced critical density ρ_c^* scales as $\lambda^{1/2}$. The compressibility factor $P_c^*/\rho_c^*kT_c^*$ at the critical point is what it is for a Lennard-Jones fluid, so that the reduced pressure P_c^* at the critical point must scale as $\lambda^{5/2}$. These results are exact and are confirmed in recent Gibbs ensemble simulations.[16]

The presence of additional dipolar or multipolar interactions however would change this to an extent determined by the strength of the dipole or quadrupole interactions. Then the law of corresponding states is not expected to hold except in special situations. For instance, the Stockmayer potential (Lennard-Jones plus point dipoles) is conformal[1,15] with the Lennard-Jones potential to $O(\mu^4)$, and the temperature-dependent effective Stockmayer potential $u^{\mathrm{ES}}(r)$ to this order is given by an equation of the same form as Eq. (3.1), i.e.,

$$u^{\mathrm{ES}}(r)=4\epsilon'[(\sigma'/r)^{12}-(\sigma'/r)^{6}], \tag{3.4}$$

with $\epsilon'=\epsilon(1+2\chi)^2$ and $\sigma'=\sigma/(1+2\chi)^{1/6}$ where $\chi(T)=\mu^{*4}/24T^*$ in which the reduced dipole moment μ^* is related to the dipole moment μ by $\mu^*=(\mu^2/\epsilon\sigma^3)^{1/2}$. A similar relationship clearly exists for systems interacting through point dipoles with the modulated Lennard-Jones potential, since the latter is conformal with the full Lennard-Jones potential. In this case, the definitions of ϵ' and σ' in the effective Stockmayer potential are altered to $\epsilon'=\epsilon(\lambda+2\chi)^2$ and $\sigma'=\sigma/(\lambda+2\chi)^{1/6}$ so that the prediction now is that the reduced critical temperature T_c^* scales as $(\lambda+2\chi)^2$ and the corresponding reduced critical density ρ_c^* scales as $(\lambda+2\chi)^{1/2}$ to $O(\mu^4)$ in the dipole moment. In the same region, the compressibility factor $P_c^*/\rho_c^*kT_c^*$ at the critical point is unchanged from that of a Lennard-Jones fluid, so that the reduced pressure P_c^* at the critical point must scale as $(\lambda+2\chi)^{5/2}$. These predictions are expected to hold only when the dipole moment μ is small. The breakdown at higher dipole moments is discussed in the Introduction.

TABLE II. Critical constants as a function of the damping factor λ in the damped Lennard-Jones model with embedded linear quadrupoles ($Q^*=2$).

λ	T_{c*}	ρ_{c*}	P_{c*}	Z_{c*}
1.0	3.965	0.424	0.455	0.2706
0.8	3.331	0.376	0.338	0.2699
0.6	2.781	0.353	0.252	0.2567
0.4	2.28	0.335	0.170	0.2226
0.2	1.861	0.299	0.118	0.2121
0.1	1.676	0.269	0.0964	0.2138
0.0	1.505	0.248	0.0768	0.2058

There is no such simplification in the thermodynamic properties of molecules with point quadrupoles added to a Lennard-Jones pair interaction and we must resort to more accurate theory or simulations to understand these systems near the critical region. Indeed, to within the accuracy of our simulations of the quadrupolar fluid when $Q^*=2.0$, our results show that the reduced critical temperature T_c^* and pressure P_c^* (Figs. 2 and 4) scale quadratically with λ; the quadratic dependence is weak, but the quality of the fit shows that it is reliable. On the other hand, the reduced critical density ρ_c^* is less reliable (Fig. 3), and appears to be adequately described by a linear dependence in λ. The compressibility factor $Z_c^*=P_c^*/\rho_c^* T_c{}^*$, which shows more scatter (Fig. 5) due to the presence of the denominator, is also adequately described by a linear dependence on λ.

IV. SUMMARY

Careful systematic study of quadrupolar damped Lennard-Jones fluid shows that the normal vapor–liquid equilibrium is observed for all values of the damping factor λ, in contrast to the equivalent dipolar case where liquid–vapor equilibrium is suppressed for $\lambda<0.35$. The scaling of the critical parameters with the damping factor λ is discussed.

ACKNOWLEDGMENTS

S.O.S. would like to thank the Natural Sciences and Engineering Research Council of Canada and the University of Lethbridge for support and facilities and J.C.R. thanks the University of Maine for support.

[1] G. Stell, J. C. Rasaiah, and H. Narang, Mol. Phys. **23**, 393 (1972); **27**, 1393 (1974).
[2] P. G. de Gennes and P. A. Pincus, Phys. Kondens. Materie **11**, 189 (1970).
[3] J. J. Weis and D. Levesque, Phys. Rev. Lett. **71**, 2729 (1993).
[4] M. E. van Leeuwen and B. Smit, Phys. Rev. Lett. **71**, 3991 (1993).
[5] G. S. Rushbrooke, G. Stell, and J. Høye, Mol. Phys. **26**, 1199 (1973).
[6] (a) D. Wei and G. N. Patey, Phys. Rev. Lett. **69**, 2043 (1992); Phys. Rev. A **46**, 7783 (1992). (b) G. Ayton and G. N. Patey, Phys. Rev. Lett. **76**, 239 (1996).
[7] M. J. Stevens and G. S. Grest, Phys. Rev. Lett. **72**, 3686 (1994).
[8] A. Z. Panagiotopoulos, Mol. Phys. **61**, 813 (1987).
[9] M. R. Stapleton, D. Tildesley, A. Z. Panagiotopoulos, and N. Quirke, Mol. Simulation **2**, 147 (1992).
[10] G. S. Dubey and S. F. O'Shea, Phys. Rev. E **49**, 2176 (1994).
[11] B. Widom, J. Chem. Phys. **39**, 2808 (1963).
[12] J. R. Recht and A. Z. Panagiotopoulos, Mol. Phys. **80**, 843 (1993).
[13] R. van Roij, Phys. Rev. Lett. **76**, 3348 (1996).
[14] S. C. McGrother and G. Jackson, Phys. Rev. Lett. **76**, 4183 (1996).
[15] J. S. Rowlinson, *Liquids and Liquid Mixtures*, 2nd ed. (Plenum, New York, 1969).
[16] S. F. O'Shea (unpublished).